Triangular grid interconnected crossed rings antenna for large-scale ultra-wideband dual polarised arrays

Yongwei Zhang[1], *Quan Shi*[1*], *Ahmed El-Makadema*[2], *Laith Danoon*[2], *Anthony K. Brown*[2]

[1] *School of Transportation, Nantong University, Nantong, China*
[2] *Department of Electrical and Electronic Engineering, School of Engineering, The University of Manchester, Oxford Road, Manchester, UK*
* *E-mail: sq@ntu.edu.cn*

Abstract: An ultra-wideband phased array antenna using interconnected elements arranged in triangular lattices is investigated. The basic unit cell of the array is a dual orthogonal crossed ring structure. Each element is interconnected to its neighbour using capacitive loading. The ring structure on a planar surface produces broad frequency bandwidth with wide scan angles. Unlike other 3-D elements such as Vivaldi antennas, the interconnected crossed ring elements can be readily configured on a triangular grid. As is well known from narrow band arrays a triangular grid allows reduction in the total number of elements needed for a given performance compared to a square grid. The array presented here applies the triangular grid to a broadband planar structure to reduce the total number of elements required by 13 percent while the electromagnetic behavior of the array is essentially maintained. An array prototype of the design has been manufactured and tested. The performance is compared to the associated array with a regular square lattice. The proposed triangular grid structure is shown to be an effective solution for applications where a minimum number of elements is required for large-scale broadband dual-polarised antenna arrays.

1 Introduction

In recent years, there has been an increasing interest in planar antenna arrays [1], particularly in large scale broadband antenna arrays such as radio astronomy [2], for their distinguishing features including easy and low-cost fabrications and low profile compared with other wideband phased array antennas such as TEM-horn [3], bunny-ear [4], body-of-revolution [5], tapered-slot, or Vivaldi [6]. Broad frequency bandwidth, wide scan angle, and dual polarisation capabilities are becoming the necessities of the latest requirements. In addition to the demand for simple construction of the arrays, geometry study is another important factor to reduce the total number of elements in the array and hence the overall cost [7].

Wideband planar arrays and their origin can be found in the continuous sheet current design introduced by Wheeler [8]. Wideband array structures have been demonstrated in practice [9][10]. Wideband performance of planar arrays with their elements arranged in a regular lattice, with or without a ground plane, has been limited by the variations in scan impedance with frequency, particularly the reactive component. Connected arrays with a ground plane have been demonstrated to produce wide bandwidth in non-scanning array but suffer poor impedance when scanned [1][11]. The idea behind this is derived from the concept of self-complementarity [12]. To overcome the scanning limitations dipoles were also connected end-to-end by using reactive loads in [10]. To increase the bandwidth Munk introduced capacitive loading between otherwise dis-connected elements [9]. This approximates the continuous current sheets as suggested by Wheeler. In Munk's design, layers of dielectric slabs on top of the array elements are important to maximise the bandwidth [13]. These layers have a number of disadvantages including the rising radio frequency loss hence increasing the antenna noise temperature.

Planar array based on Octagonal Ring Antenna (ORA) was initially investigated using two pairs of octagonal rings [2], each capacitively coupled to its neighbour, with a passive layer of rings put above the array elements, namely a meta material layer. For this antenna structure, dielectric materials are not required. To improve orthogonality between two polarisations, one significant difference of the newly proposed Crossed Octagonal Ring Antenna (C-ORA) to the initial ORA design is that there is no shared ring between the two polarisations in the C-ORA design. Most importantly, the C-ORA elements can be conveniently configured into triangular lattices other than regular square grids.

This paper explores the use of the triangular grid in reducing the number of elements in such a broadband low profile phased array whilst maintaining the other features of the capacitively interconnected design [14]. Dual polarisation requires the element to be orthogonally polarised but elements are distributed on an equilateral triangular grid. The grid configuration leads to a more complex coupling environment for the elements. This class arrays rely fundamentally on the combination of mutual coupling, together with the capacitive interconnection to provide broad bandwidth. As the triangular grid has a different coupling environment the question arises whether the bandwidth be sustained compared to the previously reported square grid.

Triangular grids themselves are not new and were reported for narrow band arrays in the 1960s [14]. In broadband applications, a Tapered-Slot Antenna array with a triangular grid is reported in [15], it is single polarised and bulky as a thick absorber is needed to suppress the backscattered field at cross-polarised incidence. An additional fibre glass layer is required at the top of array to act as a wide-angle impedance matching layer(WAIM) to improve the match in the H-plane. This approach adds loss to the system which is not acceptable in low noise applications.

A single polarised planar patch array in triangular grid is presented in [16], the frequency bandwidth and polarisation capability are both limited due to the nature of the antenna structure. On the contrary to the concept of ORA design, considerable efforts have been made to mitigate the mutual coupling among the patch elements in the planar patch array in [16]. Nevertheless, research evidence on antenna arrays of a triangular grid with ultra-wide bandwidth and dual polarisation are still scarce.

Based on the successful experience in the interconnected crossed rings array with a square grid [2][17][18], in order to use the least number of elements for maximum performance, this paper reports the triangular-grid based C-ORA array design and its performance compared to a C-ORA array with a similar element structure but arranged in a regular square grid. The unique characteristics of the

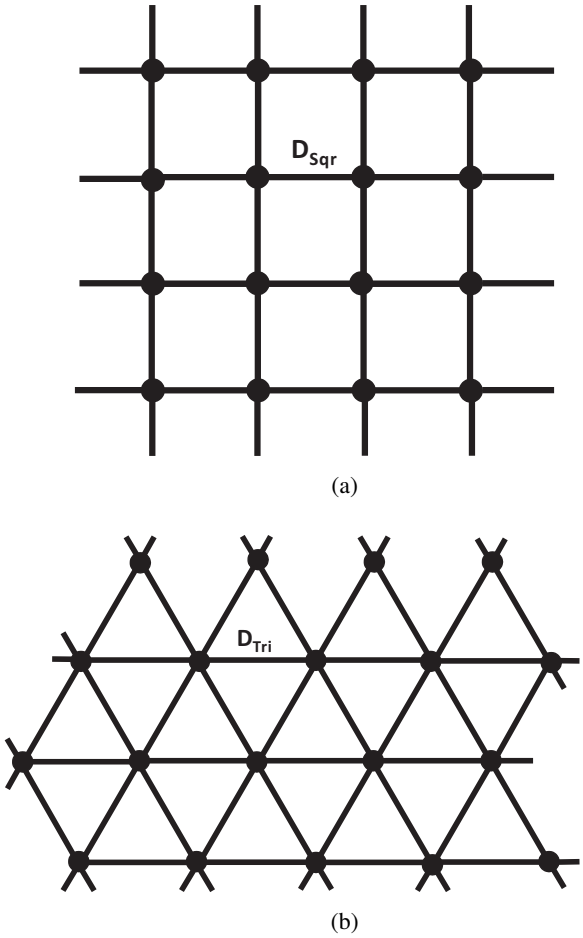

Fig. 1: *Array of elements arranged in square and triangular lattices*
(a) The square grid
(b) The triangular grid

C-ORA design, and its advantages including higher polarisation purity compared to the initial ORA design in a square grid, has been presented in [18]. In this paper, with a renewed design based on triangular grid configuration, the characteristics of the C-ORA array including broad bandwidth, dual polarisation and wide scan angle are demonstrated. The C-ORA design is easily scalable to other frequency bands hence it is well suited to other applications where a large element separation and minimum number of antenna elements are required.

2 Crossed Ring Antenna Design

For arrays with conventional elements, they can be arranged in either a square grid or a triangular grid as shown in Fig. 1. C-ORA array is a planar structure and its elements can be configured in both scenarios. However, the ground plane underneath a planar array will introduce inductance at the input terminals of the array at the low frequency. At high frequency, it tends to introduce moderate capacitance for broadside scan. In a dipole array the mutual impedance will be essentially capacitive. These are beneficial for bandwidth in a dense array based on dipole elements as a dipole element is capacitive at the low frequency and inductive at the high frequency. But for high angle scans in the E-plane, the groundplane will introduce increased inductance at the low frequency, combined with decreasing input resistance due to the opposing image effect and dominating inductance of antenna element itself at high frequency, the bandwidth of a scanning array is limited due to these factors.

C-ORA design is proposed with rings introduced close to the feeding terminals hence a self-generating capacitance within the

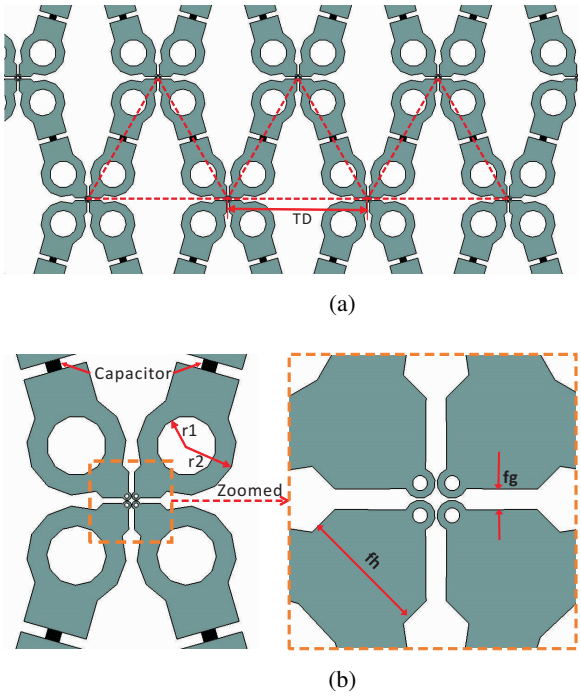

Fig. 2: *The triangular grid based C-ORA design model*
(a) Section of finite array
(b) The unit cell design mode

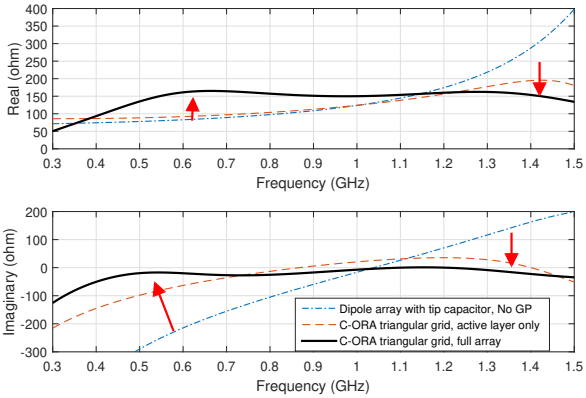

Fig. 3: *The ring effect in the C-ORA design*

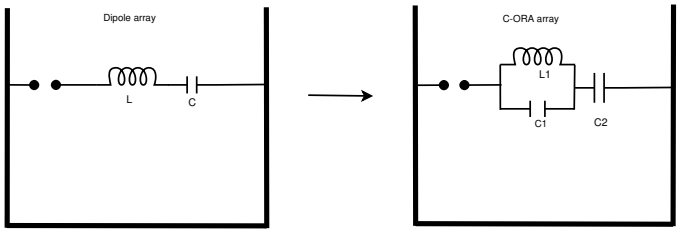

Fig. 4: *The equivalent circuit for the C-ORA, compared to the mutual coupled dipole array*

structure at the high frequency can counter the dominating inductance from the groundplane for high angle scans, especially in the E-plane. The benefits are two fold, first it can extend the scan volume; Second, it can expand the high end frequency range. A detailed C-ORA design model is illustrated in Fig. 2. The passive layer is suspended above the active layer with a specified distance, normally approximately half the distance between the active layer and the

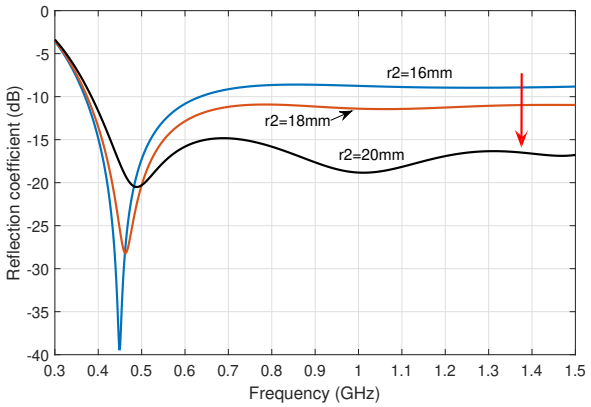

Fig. 5: *The effect of ring size on the input impedance of C-ORA elements*

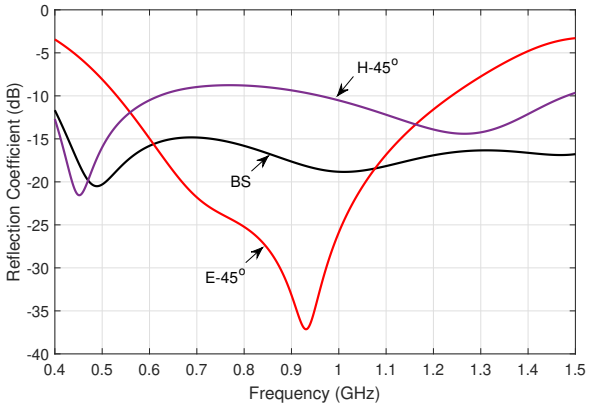

Fig. 6: *The reflection coefficients for the C-ORA based on a triangular grid*

groundplane. Due to the periodic nature of the array this passive layer forms a meta-material layer which helps maintain the input impedance of the array elements while scanning.

In this paper, the mutually coupled rings are arranged in an equilateral triangle grid to form the array. This allows the element separation to be $2/\sqrt{3}$ times of element spacing in square-grid arrays, producing the same grating lobe performance. The relationship between the element spacing for the triangular grid based array and the square grid based array is given:

$$D_{\text{Triangular}} = 2D_{\text{Square}}/\sqrt{3} \tag{1}$$

The ring effect on triangular grid based array performance can be observed from Fig. 3. The input terminals of the array elements can be made completely capacitive at the high frequency. This is of importance to counter the inductance introduced by the ground plane, especially when the array is scanned to high angles. The equivalent circuit for the C-ORA element is given in Fig. 4. Compared to the mutual coupled dipole array, an extra capacitor, with the value C1, is in parallel to the antenna self inductance close to the feed point. The size of the ring plays a significant role in improving the array performance. This is shown in Fig. 5 when the radius of ring is changing from 16mm to 20mm. According to these data, we can infer that the array tends to be resonant and narrow band when there is no rings or the ring size is small.

The active reflection coefficients of the array elements in the triangular-grid based array is shown in Fig. 6. The element separation, TD, is 121mm in the simulation. The mutual coupling between the centre element and the surrounding elements in a 16×16 finite array based on simulation is illustrated in Fig. 7. It indicates that

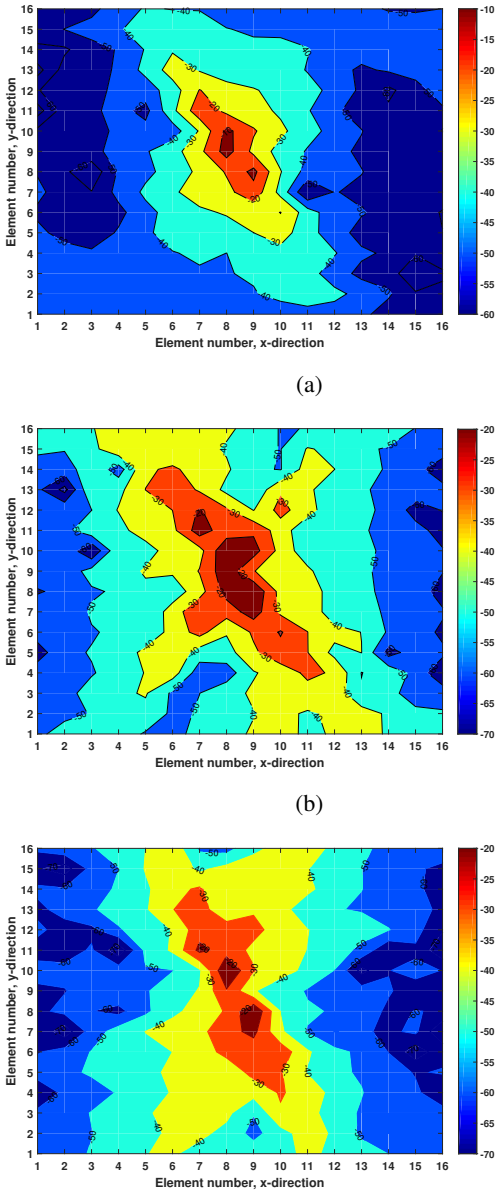

Fig. 7: *Mutual coupling between the centre element and the surrounding elements in the 16×16 finite array*
(a) 400 MHz
(b) 900 MHz
(c) 1.4 GHz

the coupling in the direction of E- or H-plane is more significant than in other orientations and it is noted that the elements are dual polarised in the $\phi = 45^o$ and $\phi = 135^o$ planes respectively in the triangular grid array. The stronger coupling at the low frequency is very important to extend the frequency bandwidth of the array. The mutual coupling between the adjacent dual polarised elements is given in Fig. 8. It is noted that the mutual coupling between the cross polarised elements is stronger in the triangular grid array than the case of a square grid. Intrinsic cross-polarization ratio (IXR) was recommended as a figure of merit (FoM) of the polarimeter [19]. It has a direct influence on the total relative error in establishing the Stokes parameters. As indicated in [20] that a reasonable requirement for IXR is 15 dB at zenith for the purposes of SKA and radio astronomy applications. The IXR for the triangular grid is acceptable for the current application. For other purposes, one possible approach to improve the polarisation isolation further is to introduce

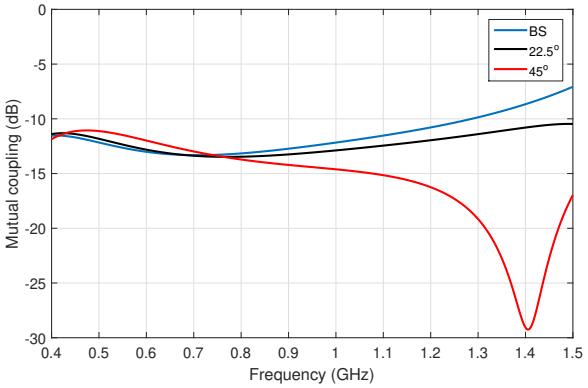

Fig. 8: *The mutual coupling between the adjacent dual polarised elements in an infinite array when it is scanned*

vertical spacing between two polarisations, i.e., etching two orthogonal polarisations on separate sides of a single planar board, with further optimisation of the interconnecting capacitor network. However for the work reported here this was not deemed a priority as the achieved performance meet the application need.

The element separation for the square based array is clearly the same in x and y directions and is 125 mm. For the triangular grid based array the separation in x becomes 144.34 mm while the y separation is maintained at 125 mm. These dimensions are chosen to allow the same scan angle for both geometries with no grating lobe production. In the triangular configuration the geometry of the crossed ring element, interconnecting capacitor and meta material layer are all re-optimised as the mutual coupling environment is significantly changed from the square grid configuration. The detailed triangular grid C-ORA design model has been illustrated in Fig. 2. The parameters of an optimised C-ORA design in a triangular grid configuration is given in Table 1.

3 Finite Array Study

3.1 Sensitivity Performance

The performance benefit of the triangular grid arrangement over the square is of great importance for many applications where the total number of array elements is the main driver of cost, particularly when the number of elements needed is very large. For example, in imaging applications such as radio astronomy [21], the total number of elements is directly related to the sensitivity figure, which is a critical parameter for the instrument. The sensitivity of an antenna array is defined as [21]

$$S = \frac{A_{\text{effective}}}{T_{\text{system}}} \tag{2}$$

Where $A_{\text{effective}}$ is the effective area of the array and T_{system} is the noise temperature of the whole system, $A_{\text{effective}}$ can be derived as

$$A_{\text{effective}} = \frac{\lambda^2}{4\pi} G \tag{3}$$

Table 1 Triangular Grid Design

Parameter	Value (mm)	Description
TD	144	Equilateral length
r1	12	Radius for inner circle
r2	20	Radius for out circle
fh	16	Width for feeding strip
fg	2.5	Gap between feeding arm

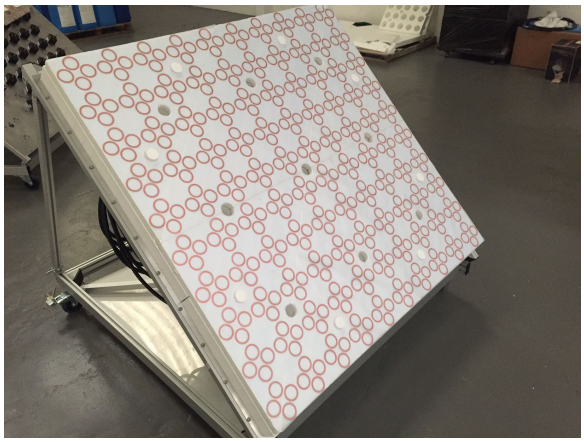

(a)

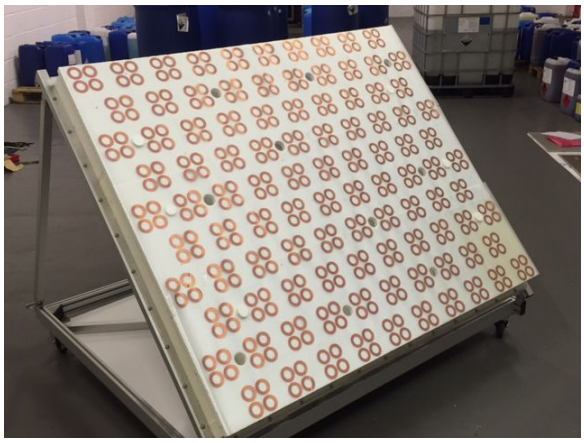

(b)

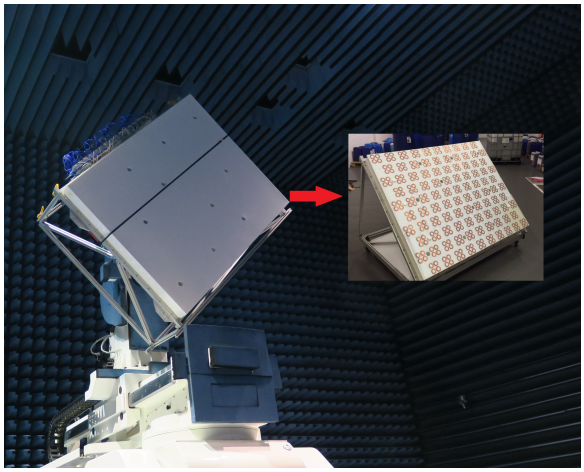

(c)

Fig. 9: *The C-ORA finite array prototypes and measurement*
(a) Square Grid C-ORA finite array
(b) Triangular Gird C-ORA finite array
(c) Triangular Grid C-ORA in the anechoic chamber

where λ is the wavelength and G is the gain of the array, and the system can be calculated by

$$T_{\text{system}} = \eta_{\text{radiation}} \cdot T_{sky} + T_0 \left(1 - \eta_{\text{radiation}}\right) + T_{\text{receiver}} \tag{4}$$

where $\eta_{\text{radiation}}$ is the radiation efficiency of the antenna, T_{sky} is the sky noise temperature, T_0 is the antenna noise temperature and T_{receiver} is the receiver noise temperature. The sensitivity of the

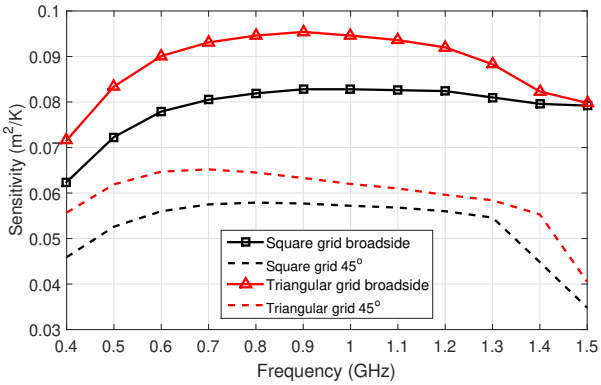

Fig. 10: *The comparison of sensitivity of the 16×16 C-ORA finite arrays in square and triangular grid, simulated*

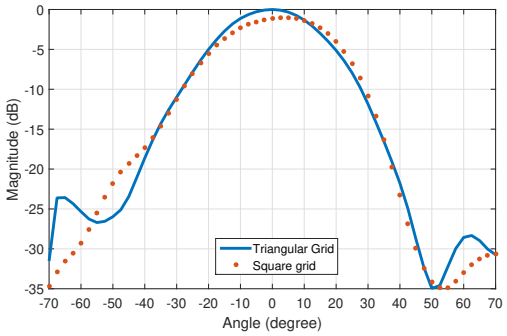

(a)

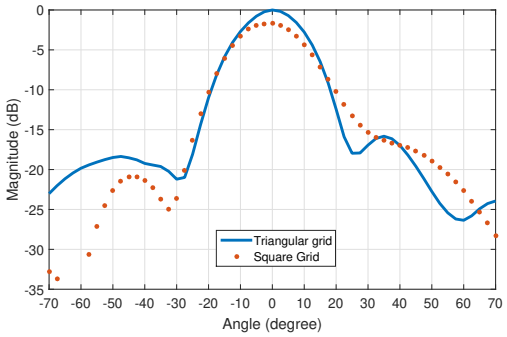

(b)

Fig. 11: *The relative gain comparison of triangular and square grid based subarrays with 4×4 elements, measured in the D-plane for both configurations*

(a) 900 MHz
(b) 1.4 GHz

finite arrays with a square grid and triangular grid is illustrated in Fig. 10. A significant increase was observed for the array with a triangular grid for scans both at the zenith and 45^o. Overall it is in good alignment with the fact that the triangular grid array covers 12.7% more physical collecting area than the subarray of a square grid. The results confirm that the triangular grid C-ORA array can produce the same sensitivity with a square grid based array, but with approximately 13% less total number of elements. In addition to the advantage on the element number reduction which is the focus of this paper, other characteristics of the proposed planar array were compared with two other SKA candidate antennas in [22].

For application such as the SKA mid-frequency array, the required sensitivity is 10,000 m^2/K at the frequency of 800 MHz [21]. The number of elements needed to achieve this performance

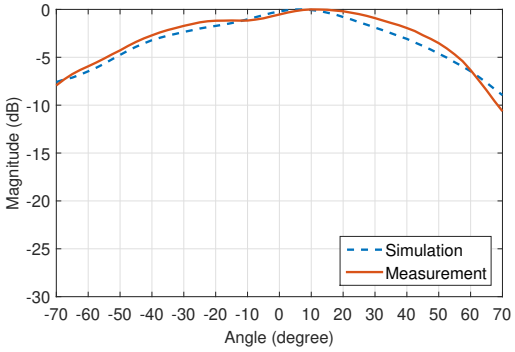

(a)

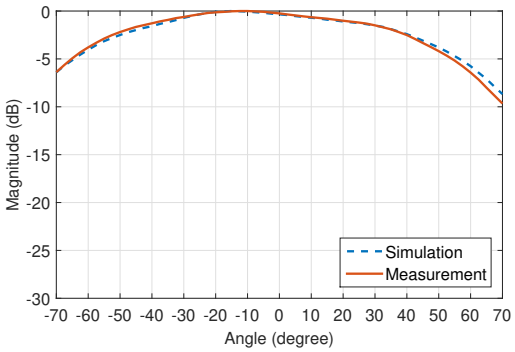

(b)

Fig. 12: *The radiation patterns of the immersed centre element of the finite triangular grid C-ORA array*

(a) 600MHz, E-plane
(b) 600MHz, H-plane

in a square grid is 25.3 M. Using a triangular grid, the number of elements needed for the same sensitivity is 22 M, reducing the total number of elements by 3.3M [23]. This investigation proves that the C-ORA design with elements arranged on a triangular grid is a robust solution for such application.

3.2 Radiation Pattern

10×10 finite array based on triangular grid was manufactured for measurements as depicted in Fig. 9. In order to compare its performances to a regular square based array, a 10×10 finite array based on the square grid was also manufactured using C-ORA elements optimised for the square grid configuration of exactly the same number of elements. A 4×4 analogue beamformer was used to measure the radiation patterns of subarrays for both structures. Only the broadside performances were able to be measured as the power divider network used was unable to scan the array. The synthesized Co-Pol patterns for both 4×4 subarrays are shown in Fig. 11. A higher gain for the triangular grid based array is observed – approximately 1 dB with the same number of elements from the 4×4 subarrays. This agrees with the theory that the effective array antenna aperture, A_e, is proportional to the gain of the array as shown in (3). The effective aperture of the triangular grid based array covers 12.7% more physical area than the square grid based array. It corresponds to slightly more than 1dB in energy collection. The relative gain of the subarray of the triangular grid compared to that in the square grid is summarised in Table 2. It confirmed that the gain for the triangular grid based array is greater than that for square based array by using the same number of elements. The immersed element pattern of the centre element in the finite array was measured. A good agreement between the measured results and the simulation is achieved. Measured radiation patterns for the centre element of the finite array with a triangular grid at 600MHz and 1.4GHz are shown in Fig. 12 and

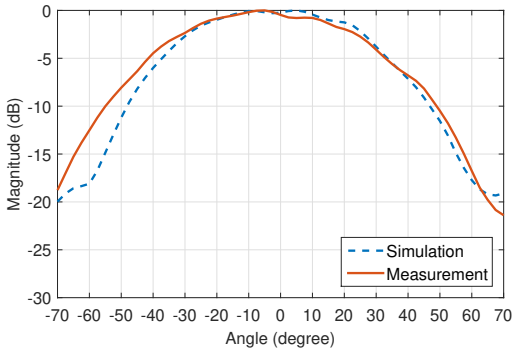

(a)

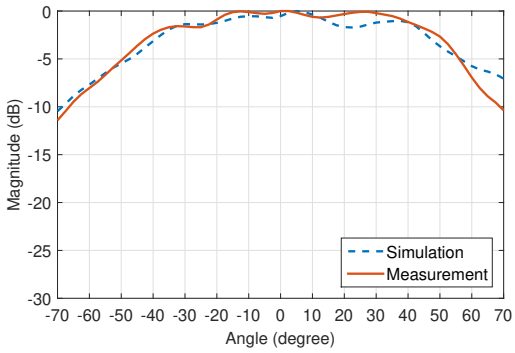

(b)

Fig. 13: *The radiation patterns of the immersed centre element of the finite triangular grid C-ORA array*
(a) 1.4 GHz, E-plane
(b) 1.4 GHz, H-plane

Table 2 Relative gain for triangular array compared to the square array

Frequency(GHz)	Relative gain of triangular grid to square grid (dB)	Notes
0.6	0.5	Poor matching
0.9	1	
1	1.2	
1.1	1	
1.2	0.9	
1.3	0.8	
1.4	1.6	

Fig. 13 respectively. In general the pattern in the H-plane is broader than that in the E-plane for both arrays. This is a typical characteristic of dipole types of antennas. The scan range of $\pm 45^{\circ}$ from the zenith can be achieved across the frequency range up to 1.45GHz.

4 Conclusion

The triangular grid based C-ORA study demonstrates its ability in dual polarised wide band array applications. Most importantly, to achieve the same sensitivity, the greater element separation of such design can reduce the total number of elements by 13% compared with the square-grid based arrays. This can be achieved without sacrificing the side lobe level performance. The array structure is planar with minimum dielectric materials needed to achieve the performance so is inherently a low loss design. This flexibility in adopting different grid geometries is not readily available from other popular broad band array antennas. It is particularly significant for large-scale applications such as in radio astronomy. The simple planar structure design with few parameters to define the element design makes it convenient for wide band applications where a large element spacing is desired.

5 Acknowledgments

The authors would like to thank STFC UK for the support of the SKA project, and editors and reviewers for their valuable comments to improve the quality of the paper.

6 References

[1] Hansen, R.: 'Phased array antennas' (Wiley, 2009, 2nd edn., in Wiley series in microwave and optical engineering)

[2] Zhang, Y., Brown, A. K.: 'Octagonal Ring Antenna for a Compact Dual-Polarized Aperture Array', IEEE Transactions on Antennas and Propagation, 2011, 59, (10), pp. 3927–3932

[3] Holzman, E. L.: 'A wide band TEM horn array radiator with a novel microstrip feed'. Proc. 2000 IEEE International Conference on Phased Array Systems and Technology, May 2000, pp. 441–444

[4] Lee, J. J., Livingston, S. and Koenig, R.: 'A low-profile wide-band (5:1) dual-pol array', IEEE Antennas and Wireless Propagation Letters, 2003, 2, (1), pp. 46–49

[5] Holter, H.: 'Dual-Polarized Broadband Array Antenna With BOR-Elements, Mechanical Design and Measurements', IEEE Transactions on Antennas and Propagation, 2007, 55, (2), pp. 305–312

[6] Schaubert, D. H., Kasturi, S., Boryssenko, A. O., et al.: 'Vivaldi Antenna Arrays for Wide Bandwidth and Electronic Scanning'. Proc. The Second European Conference on Antennas and Propagation, EuCAP 2007, Nov 2000, pp. 1–6

[7] El-makadema, A., Rashid, L., Brown, A. K.: 'Geometry Design Optimization of Large-Scale Broadband Antenna Array Systems', IEEE Transactions on Antennas and Propagation, 2014, 62, (4), pp. 1673–1680

[8] Wheeler, H.:'Simple relations derived from a phased-array antenna made of an infinite current sheet', IEEE Transactions on Antennas and Propagation, 1965, 13, (4), pp. 506–514

[9] Munk, B. A.: 'Finite Antenna Arrays and FSS' (Wiley-IEEE Press, 2003)

[10] Hansen, R. C.: 'Non-Foster and connected planar arrays', Radio Science, 2004, 39, (4), pp. 1–14

[11] Hansen, R. C.: 'Linear connected arrays [coupled dipole arrays]', IEEE Antennas and Wireless Propagation Letters, 2004, 3, pp. 154–156

[12] Inagaki, N., Isogai, Y., Mushiake, Y.: 'Ichimatsu Moyou antenna - Self-complementary antenna with periodic feeding points', Electronics Communications of Japan, 1979, 62, pp. 52–60

[13] Munk, B., Taylor, R., Durharn, T. et al.: 'A low-profile broadband phased array antenna'. Proc. IEEE Antennas and Propagation Society International Symposium. Digest. Held in conjunction with: USNC/CNC/URSI North American Radio Sci. Meeting (Cat. No.03CH37450), 2003, pp. 448–451

[14] Sharp, E.: 'A triangular arrangement of planar-array elements that reduces the number needed', IRE Transactions on Antennas and Propagation, 1961, 9, (2), pp. 126–129

[15] Ellgardt, A., Wikstrom, A.: 'A Single Polarized Triangular Grid Tapered-Slot Array Antenna', IEEE Transactions on Antennas and Propagation, 2009, 57, (9), pp. 2599–2607

[16] Abbasi Arand, B., Bazrkar, A., Zahedi, A.: 'Design of a Phased Array in Triangular Grid With an Efficient Matching Network and Reduced Mutual Coupling for Wide-Angle Scanning',

IEEE Transactions on Antennas and Propagation, 2017, 65, (6), pp. 2983–2991

[17] de Vaate, J. G. B. et al.: 'SKA Mid Frequency Aperture arrays: Technology for the ultimate survey machine', 2014 XXXIth URSI General Assembly and Scientific Symposium (URSI GASS), Beijing, 2014, pp. 1–4

[18] Zhang, Y., Brown, A. K.: 'A Wideband Planar Aperture Array Using Interconnected Crossed Rings', IEEE Transactions on Antennas and Propagation, 2019, 67, (2), pp. 945–950

[19] Carozzi, T. D., Woan, G.: 'A fundamental figure of merit for radio polarimeter', IEEE Transactions on Antennas and Propagation, 2011, 59, pp. 2058–2065

[20] Fiorelli, B., de Lera Acedo, E.: 'Polarization performance of the SKA Low Frequency Aperture Array station', 2014 International Conference on Electromagnetics in Advanced Applications (ICEAA), Palm Beach, 2014, pp. 726–729

[21] Faulkner, A., Kant, D., Alexander, P. et al.: 'The Aperture Arrays for the SKA: the SKADS White Paper', SKA memo 122, Dec 2010

[22] Zhang, Y., Brown, A. K.: 'Design of Wide-Band Dual Polarized Aperture Array Antennas', International Journal of Microwave and Wireless Technologies, 2012, Vol. 4, Special Issue 3, pp. 373–378

[23] Zhang, Y., El-Makadema, A., de Lera Acedo, E. et al.: 'On the front-end design of mid-frequency aperture array for square Kilometre array', Experimental Astronomy, 2018, 46, (2), pp. 357–380